Original Research

Nonlinear Myocardial Signal Intensity Correction Improves Quantification of Contrast-Enhanced First-Pass MR Perfusion in Humans

Li-Yueh Hsu, DSc,* Peter Kellman, PhD, and Andrew E Arai, MD

Purpose: To study the nonlinearity of myocardial signal intensity and gadolinium contrast concentration during first-pass perfusion MRI, and to compare quantitative perfusion estimates using nonlinear myocardial signal intensity correction.

Materials and Methods: The nonlinearity of signal intensity and contrast concentration was simulated by magnetization modeling and evaluated in phantom measurements. A total of 10 healthy volunteers underwent rest and stress dual-bolus perfusion studies using an echo-planar imaging sequence at both short and long saturation-recovery delay times (TD70 and TD150). Perfusion estimates were compared before and after the correction.

Results: The phantom data showed a linear relationship (R^2 = 1.00 and 0.99) of corrected signal intensity vs. contrast concentrations. Peak myocardial contrast concentration averaged 0.64 ± 0.10 mmol · L^{-1} at rest and 0.91 ± 0.21 mmol · L^{-1} during stress for TD70 and were similar for TD150 (P = not significant [NS]). The corrections were larger for stress than rest perfusion and larger for TD150 than TD70 studies (both $P < 0.01$). Perfusion estimates of TD70 and TD150 stress studies were significantly different before the correction ($P < 0.01$) but equivalent after the correction (P = NS).

Conclusion: The nonlinearity between signal intensity and myocardial contrast concentration in perfusion MRI can be corrected through magnetization modeling. A nonlinear correction of myocardial signal intensity is feasible and improves quantitative perfusion analysis.

Key Words: myocardial perfusion; myocardial blood flow; myocardial perfusion reserve; contrast agent; gadolinium; dipyridamole
J. Magn. Reson. Imaging 2008;27:793–801.

Laboratory of Cardiac Energetics, National Heart Lung and Blood Institute, National Institutes of Health, Department of Health and Human Services, Bethesda, Maryland, USA.

Contract grant sponsor: National Heart, Lung, and Blood Institute.

*Address reprint requests to: L.-Y.H., DSc, Laboratory of Cardiac Energetics, National Heart, Lung, and Blood Institute, National Institutes of Health, 10 Center Dr., MSC 1061, Building 10, Room B1D-416, Bethesda, MD 20892-1061. E-mail: lyhsu@nhlbi.nih.gov

Received January 30, 2007; Accepted December 3, 2007.
DOI 10.1002/jmri.21286
Published online 26 February 2008 in Wiley InterScience (www.interscience.wiley.com).

QUANTITATIVE ANALYSIS of myocardial perfusion using first-pass contrast-enhanced MRI is useful for detecting coronary artery disease (1–9), assessing therapeutic intervention (10–13), and predicting risk of coronary artery disease in asymptomatic adults (14,15). Myocardial blood flow (MBF) and myocardial perfusion reserve (MPR) can be estimated from changes between myocardial time signal intensity curves obtained at rest and during stress. However, the nonlinear relationship between myocardial signal intensity and gadolinium contrast concentration in MR perfusion imaging is an important issue that might affect analysis of myocardial perfusion (16,17).

Despite many efforts focused on improving the linearity of the left ventricular (LV) blood pool signal intensity, relatively little work has been published with regard to improving the nonlinearity in the myocardium. Various imaging techniques have been published to maintain the linearity of the LV blood pool signal intensity, including dual-bolus (18,19), prebolus (20,21), and dual-sequence (22,23) methods. These methods either use a low-dose bolus (18–21) or combine short echo time and short delay time (TD) (22,23) to optimize the dynamic range of the acquisition for peak contrast concentration and thus maintain the linearity of the LV signal intensity. An alternative approach is using postimaging signal intensity calibration such as in vitro phantom-based (24) or in vivo image theory-based (16) methods to compensate for signal distortion at peak contrast due to the T1 shortening.

A recent healthy volunteer study (17) has shown the signal intensity increased proportionally with gadolinium contrast concentrations up to 0.05 mmol/kg in the myocardium. However, previous multicenter clinical studies (25,26) have reported that using a higher dose (0.1–0.15 mmol/kg) of gadolinium contrast demonstrated a higher diagnostic performance in detecting coronary artery stenoses than using a lower one (0.05 mmol/kg). It may be advantageous to use a high dose of contrast and employ a nonlinear postimaging signal intensity correction scheme for analyzing MR perfusion images.

The aim of this study is to examine the nonlinear relationship of signal intensity vs. myocardial contrast concentration using a high dose (0.1 mmol/kg) of gad-

olinium-diethylene triamine pentaacetic acid (Gd-DTPA) for first-pass perfusion MRI on healthy volunteers during stress and at rest. The nonlinearity of the signal intensity is simulated based on magnetization modeling, which allows estimation of myocardial gadolinium concentration as a function of time. Applying a nonlinear correction to the myocardial time signal intensity curves, we determine how this nonlinearity affects quantitative perfusion estimates at different imaging parameter (saturation-recovery TD) settings.

MATERIALS AND METHODS

Magnetization recovery of a saturation preparation perfusion sequence was simulated to study the nonlinearity between signal intensity and gadolinium contrast concentration. Signal intensity of arbitrary units was converted to gadolinium contrast concentration estimates in units of millimoles per liter (mmol $\cdot$ L^{-1}), based on the magnetization modeling. The accuracy of the simulation was evaluated in a T1 phantom of different contrast concentrations. The nonlinear relationship was applied to perfusion MRI of 10 healthy volunteers at rest and during stress to correct myocardial time signal intensity curves. The degree to which this nonlinearity affected quantitative myocardial perfusion estimates was assessed using two different imaging protocols (two saturation-recovery TDs).

Nonlinear Signal Intensity Correction

The relationship of signal intensity vs. T1 magnetization was simulated based on a saturation prepared echo-planar imaging sequence (27). The simulation was implemented in Matlab (The MathWorks, Natick, MA, USA) and using actual sequence parameters in the perfusion imaging. This T1 modeling is similar to the work of Cernicanu and Axel (16) except our simulation is based on the theoretical development of Sekihara (28).

Assume M_n^- and M_n^+ are the magnetization vectors of each spin isochromat just before and after the nth application of the radio frequency (RF) pulse. Their relationship can be expressed as

$$M_n^+ = R_x(\alpha) \cdot M_n^-, \qquad [1]$$

where R_x is the rotation operator about the x-axis and α is the readout flip angle. Next, the relationship between M_n^+ and M_{n+1}^- can be expressed as

$$M_{n+1}^- = R_z(\theta_n) \cdot \begin{bmatrix} e^{-TR/T_2} & 0 & 0 \\ 0 & e^{-TR/T_2} & 0 \\ 0 & 0 & e^{-TR/T_1} \end{bmatrix} \cdot M_n^+ + (1 - e^{-TR/T_1}) \cdot M_0, \qquad [2]$$

where R_z is the rotation operation about the z-axis, θ_n is the phase rotation during the period between the nth and $(n+1)$th RF pulses, TR is the repetition time of the RF pulse, and $M_0 = [0, 0, M_0]$ is the magnetization vector in thermal equilibrium.

The formulation of the initial magnetization vector was modified to incorporate a saturation pulse with specified trigger time delay TD

$$M_1^- = R_x(\alpha) \cdot e^{-TD/T_1} \cdot M_0 + (1 - e^{-TD/T_1}) \cdot M_0. \qquad [3]$$

The magnetization of the RF pulse was calculated assuming a uniform distribution of isochromats θ_n within a voxel according to the method of Sekihara (28). The magnetization vectors of such voxel before and after the nth RF pulse $\hat{M}_n^-$ and $\hat{M}_n^+$ can be expressed as

$$\hat{M}_n^- = (\hat{M}_x^-, \hat{M}_y^-, \hat{M}_z^-) = \int_0^{2\pi} M_n^-(\theta_{n-1}) d\theta_{n-1}, \qquad [4]$$

$$\hat{M}_n^+ = (\hat{M}_x^+, \hat{M}_y^+, \hat{M}_z^+) = \int_0^{2\pi} M_n^+(\theta_{n-1}) d\theta_{n-1}. \qquad [5]$$

The magnetization of each image was computed based on the center of k-space after reordering the phase-encode direction according to the modified center-out acquisition (27).

In order to be independent of actual proton density (PD) and surface coil profile, an additional magnetization vector was calculated using a small readout flip angle and without saturation-recovery preparation in the sequence parameters. The simulated signal intensity value was derived using the T1-weighted transverse magnetization normalized (divided) by the PD-weighted transverse magnetization. Assuming a constant myocardial T2 value of 50 msec (29), this simulated signal intensity was calculated over a range of T1 values.

The relationship of T1 value vs. gadolinium contrast concentration was estimated using the equation

$$1/T_1 = 1/T_1^0 + \gamma \cdot [Gd], \qquad [6]$$

where T_1^0 is the myocardium precontrast T1 value, which is assumed to be 850 msec, γ is the relaxivity of gadolinium (Gd-DTPA) contrast, which equals 4.5 L $\cdot$ mmol^{-1} $\cdot$ second^{-1} (30), and $[Gd]$ is the concentration of Gd in mmol $\cdot$ L^{-1}. In this manner, a nonlinear relationship that maps the simulated signal intensity to a range of myocardial contrast concentration encountered during first-pass perfusion was derived. Since precontrast T1 and T2 values may vary in the heart, a range of precontrast T1 and T2 values was also studied by the simulation to analyze the sensitivity to the nonlinearity.

To apply this nonlinear relationship for signal intensity correction, normalized signal intensity values were calculated using the signal intensity measurements in the T1-weighted image divided by the corresponding signal intensity measurements in the PD reference image, where measurements corresponded to regions of interest. This yielded the normalized signal intensity in either relaxivity (R1) or contrast concentration ($[Gd]$) units and derived a linear relationship of corrected signal intensity vs. contrast concentration.

To compare the corrected myocardial time signal intensity curves of the perfusion image with the raw

curves, final corrected myocardial time signal intensity curve *SI* was derived by linearly scaling of the time contrast concentration curve [*Gd*] using the equation

$$SI = S \cdot [Gd] + I, \quad [7]$$

where *S* and *I* were computed using the myocardial signal intensity and contrast concentration measurements at PD reference and precontrast baseline time points.

Imaging Sequence

Perfusion imaging was performed on a 1.5-T Siemens Espree scanner (Siemens Medical Solutions, Erlangen, Germany) using a gradient recalled echo–echo planar imaging (GRE-EPI) sequence (27) with a 12-element phased-array Siemens torso coil. The following parameters were used to collect the dynamic series of T1 images: saturation preparation = 90°, readout flip angle = 25°, TR = 7.5 msec, TE = 1.48 msec, slice thickness = 8 mm, echo train length = 4, acquisition matrix = 128 × 80–96, field of view (FOV) = 360 × 270 mm, and parallel imaging with rate 2 temporal sensitivity encoding (TSENSE) (31). Chemical shift fat suppression was applied during the saturation-recovery period to reduce EPI ghosting artifacts. A short saturation-recovery TD (70 msec) and a long saturation-recovery TD (150 msec) were used to compare the effect of nonlinear signal intensity correction. These TDs were selected as spanning a typical range used in recent perfusion studies (10,17,25,26).

At the start of each perfusion acquisition, two PD-weighted reference images were acquired for intensity normalization using the same imaging parameters except no saturation preparation pulse and using a 5° readout flip angle. With a full resolution of 80 phase-encode lines and rate 2 SENSE factor, 40 phase-encode lines were collected from 10 shots, which put the acquisition of the center of k-space at approximately 35 msec after the trigger delay. This resulted in a total time to the center of k-space at 105 msec and 185 msec for TD70 and TD150, respectively. In addition to the actual saturation-recovery TD used, simulation was also performed at a shorter TD (25 msec) to cover a wider range of parameters for comparing the nonlinearity between signal intensity and gadolinium contrast concentration.

In Vitro Study

In order to validate the accuracy of the nonlinear signal intensity correction, a phantom consisting of 10 concentrations (0.16–2.35 mmol · L^{-1}) of Gd-DTPA (Magnevist; Berlex Laboratories, Wayne, NJ, USA) was prepared in saline-filled plastic tubes to cover the anticipated range of T1 values in the myocardium during the perfusion imaging. The T1 and T2 values of the phantom were measured using standard inversion-recovery (TR = 750–1000 msec, TE = 2.45 msec, TI = 100–980 msec) and spin-echo (TR = 3000 msec, TE = 20–600 msec) imaging sequences of the scanner. The PD reference and T1 series images were collected using the same GRE-EPI perfusion sequence parameters described previously at both TD70 and TD150 settings. Circular regions of interest were drawn inside the tubes to measure signal intensities. Signal intensity measurements of the regions of interest before and after the correction were compared. Linear correlations were computed between the corrected signal intensity and contrast concentrations.

In Vivo Study

In order to assess the effect of signal intensity correction on quantitative myocardial perfusion estimates, 10 healthy volunteers (six men and four women, mean age 40 ± 9, 10-year risk of coronary heart disease <2% based on the Framingham score) each went through rest and dipyridamole stress perfusion scans at both TD70 and TD150 settings. Written informed consent was obtained from all subjects. All studies were performed under procedures and protocols approved by the Institutional Review Board of the National Institutes of Health. Using a dual-bolus perfusion imaging protocol (18), two doses of Gd-DTPA at 0.005 mmol · kg^{-1} and 0.1 mmol · kg^{-1} were prepared in equal volumes and injected at 5 mL · $second^{-1}$. Rest perfusion was performed at least four hours after the stress study in which 0.56 mg · kg^{-1} of dipyridamole was infused over four minutes. The TD70 and the TD150 imaging were performed on separate days. For each perfusion acquisition, two short-axis slices and 60 images per slice were collected in a single breathhold and at every heartbeat using the previously described GRE-EPI sequence parameters.

Data Analysis

The endocardial and epicardial borders of the perfusion images were manually traced and registered using Argus cardiovascular MR software (Siemens Medical Solutions, Erlangen, Germany). The myocardial regions of interest were divided into six circumferential sectors at each slice location. Time signal intensity curves of the blood cavity and the myocardial sectors were generated from both low-concentration and high-concentration images, respectively, after using the PD reference signal intensity for surface coil intensity normalization.

The myocardial perfusion estimates were compared from these time signal intensity curves before and after the nonlinear signal intensity correction using custom software written in Interactive Data Language (ITT Visual Information Solutions, Boulder, CO, USA). The following measurements, as described in previous works (19,32), were computed: semiquantitative MBF indices (MBFi) based on intensity upslope (SLP) and contrast enhancement ratio (CER); and fully quantitative MBF estimate based on a Fermi model-constrained deconvolution (MCD). MPR and MPR index (MPRi) were calculated as a ratio of stress divided by rest MBF and MBFi. The same timing parameters were used to quantify the myocardial time signal intensity curves before and after the nonlinear correction.

Peak myocardial contrast concentration estimated from TD70 and TD150 perfusion studies were com-

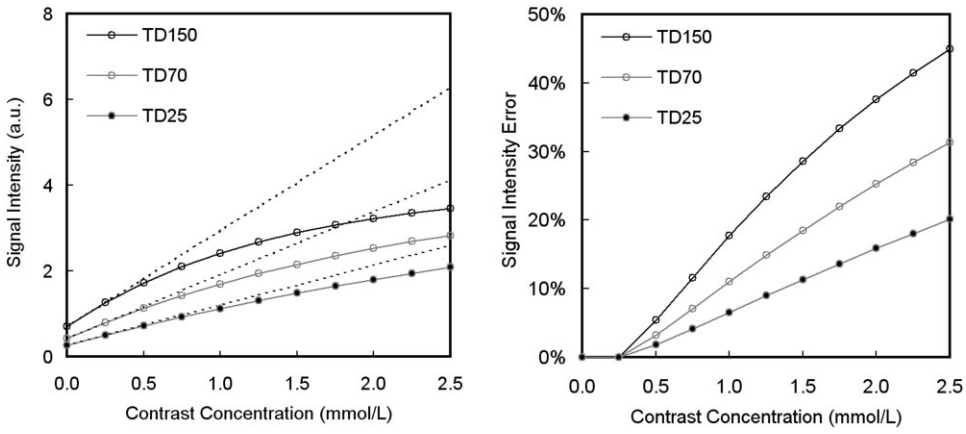

Figure 1. Simulations showing the nonlinearity of signal intensity (left) and signal intensity error (right) as a function of contrast concentration at different TD settings. Dashed lines in the left plot show the reference linear relationship between signal intensity and contrast concentration that were linearly extrapolated using the first two points. The nonlinearity is more severe for longer TDs and results in larger signal intensity errors, as shown in the right plot.

pared using linear correlations. Results were expressed as mean ± standard deviation (SD). Magnitude of change of the perfusion estimates after the signal intensity correction was reported for MBF and MBFi estimates at rest, during stress, and for MPR and MPRi. Statistical differences were identified with a paired Student's *t*-test for all comparisons.

RESULTS

Figure 1 shows the nonlinear relationship between simulated signal intensity and gadolinium contrast concentration based on the actual perfusion sequence and acquisition parameters. Saturation-recovery TD25, TD70, and TD150 were compared in the simulations. The signal intensity vs. contrast concentration curve is more nonlinear for longer saturation-recovery TD, but longer TD achieves a higher signal intensity magnitude (signal-to-noise ratio, SNR). The magnitude of signal intensity error (compression) was 6.6%, 11.0%, and 17.7% for TD25, TD70, and TD150 at 1.0 mmol · L^{-1} of contrast concentration. Compared with TD25, the signal intensity of TD70 was 1.5 times higher and the signal intensity of TD150 was 2.2 times higher for contrast concentration at 1.0 mmol · L^{-1}, illustrating the tradeoffs between SNR and linearity.

Figure 2 shows the simulation of how the nonlinear relationship between signal intensity and contrast concentration varies as a function of precontrast T1 and T2 values that may encountered in the heart. As expected for a heavily T1-weighted sequence with minimal T2 weighting, the effect of precontrast T2 value was minimal in the range that was simulated (20–200 msec). The relationship of signal intensity vs. contrast concentration is slightly more linear using a precontrast T1 value of normal myocardium (850 msec) than the blood (1200 msec). However, the effect of precontrast T1 values in changing the nonlinearity becomes more prominent as the value approaches 600 msec.

In Vitro Studies

The T1 values of the phantom ranged from 91 to 914 msec for various Gd-DTPA concentrations. Figure 3 shows that the nonlinear signal intensity correction effectively restored a linear relationship between signal intensity and contrast concentration. Good linear correlations between the corrected signal intensity and the contrast concentration were obtained at both TD70 and TD150 (R^2 = 1.00 and 0.99, respectively). The signal intensity of TD150 after the correction showed slightly less-than-perfect linear correspondence at the very high contrast concentration (T1 = 91 msec) perhaps since the magnitude of signal intensity compression was significantly larger and thus more sensitive to noise.

In Vivo Studies

All subjects went through the studies without adverse events. The average heart rate was 61 ± 11 bpm for the rest perfusion study and increased to 92 ± 10 during the dipyridamole stress test ($P < 0.01$). The systolic blood pressure averaged 113 ± 10 at rest and 119 ± 19 during stress; and the diastolic blood pressure did not change from 69 ± 8 at rest to 70 ± 10 during stress (both P = not significant [NS]).

Figure 4 shows examples of TD70 and TD150 images from a healthy volunteer. The TD150 images showed higher myocardial signal intensity than the corresponding TD70 ones. Figure 5 compares the time signal intensity curves of a myocardial sector before and after the correction at both TD70 and TD150 settings. The largest effect of signal intensity compression was around the peak of myocardial contrast enhancement. The TD150 required more correction than the corresponding TD70 studies.

Figure 6 shows the correlation of peak estimated myocardial contrast concentration between TD70 and TD150 studies. Bland-Altman analysis shows no consistent difference between peak concentration estimates for both TDs. Peak myocardial contrast concentration at rest perfusion was estimated at 0.64 ± 0.10 mmol · L^{-1} for TD70 and 0.61 ± 0.11 mmol · L^{-1} for TD150 (P = NS), and during stress perfusion was 0.91 ± 0.21 mmol · L^{-1} for TD70 and 0.84 ± 0.16 mmol · L^{-1} for TD150 (P = NS). Peak myocardial contrast concentration estimates varied from 0.39 to 0.71 mmol · L^{-1} at rest perfusion and increased to a larger degree from 0.77 to 1.32 mmol · L^{-1} during stress perfusion ($P < 0.01$).

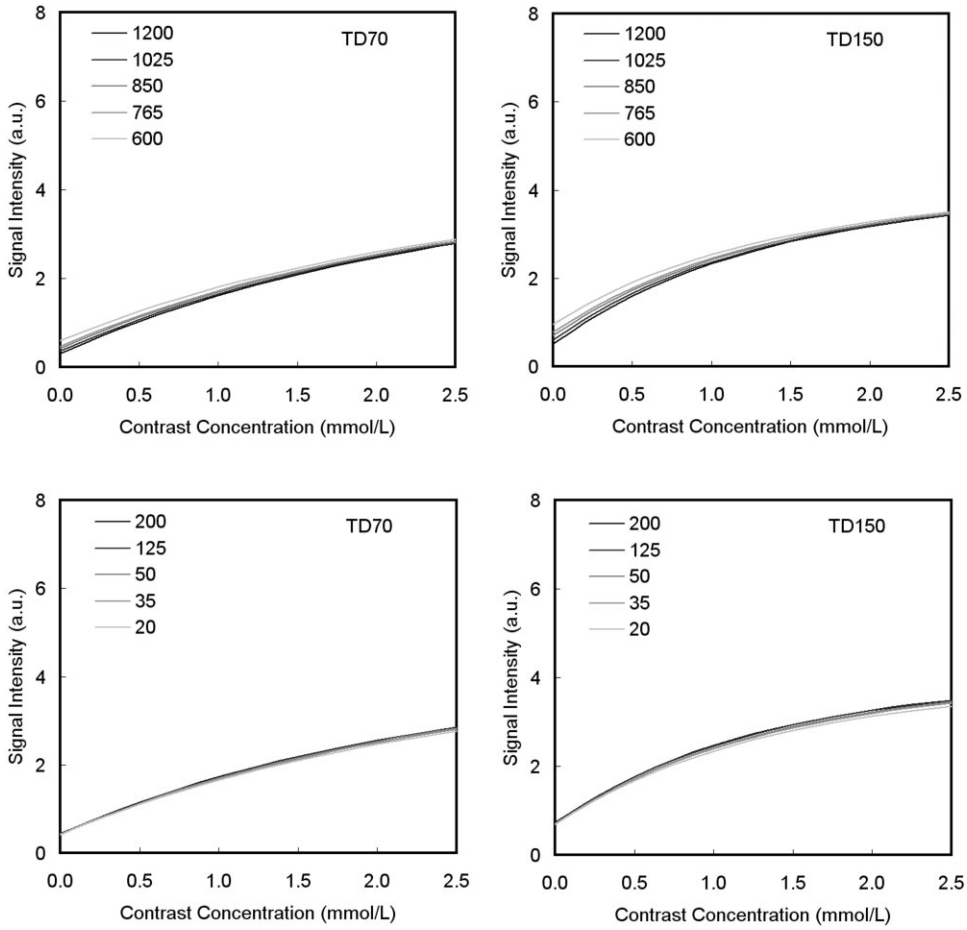

Figure 2. The effect of precontrast T1 and T2 values on the nonlinear relationship between signal intensity and gadolinium concentration was simulated. Precontrast T1 had mild effects within a range from 1200 msec to 850 msec using a fixed T2 at 50 msec (top row). Precontrast T2 had minimal effects over a range from 200 msec to 20 msec using a fixed precontrast T1 at 850 msec (bottom row). Similar results were seen in both TD70 (left) and TD150 (right) simulations.

Effect of Nonlinear Signal Intensity Correction on Perfusion Quantification

For intrasubject comparison of myocardial perfusion estimates between TD70 and TD150 studies, Figure 7 shows that quantitative stress MBF and MPR estimated by Fermi MCD were significantly smaller for TD150 than for TD70 studies before the signal intensity correction ($P < 0.01$), but this difference became insignificant after the correction (P = NS). Rest MBF estimate remained similar before or after the correction for both TDs (P = NS).

Figure 8 shows the magnitude of change of semiquantitative and fully-quantitative myocardial perfusion estimates after the nonlinear signal intensity correction. The magnitude of change for each perfusion estimate is listed above each bar in Figure 8. Semiquantitative MBFi and MPRi by CER and SLP, and fully-quantitative MBF and MPR by MCD all increased after the correction (all $P < 0.01$). All rest perfusion estimates had smaller increase compared with the corresponding stress measures for both TDs ($P < 0.01$). All TD70 perfusion estimates had smaller

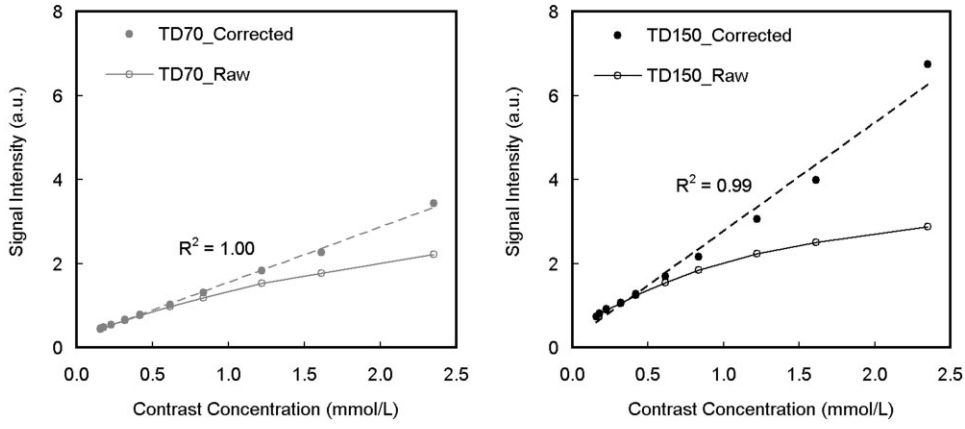

Figure 3. Signal intensity vs. contrast concentration plots of the T1 phantom data show that the correction can recover the nonlinear signal intensity of different contrast concentrations to a linear relationship. Dashed lines indicate the linear fit of the signal intensities after the nonlinear correction.

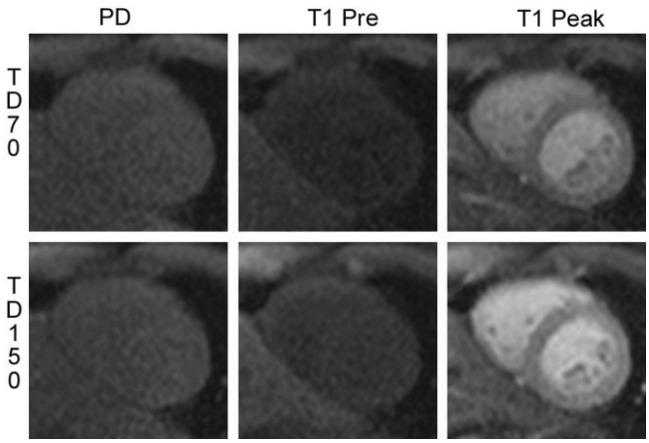

Figure 4. Example images show that the T1-weighted image of TD150 study at peak contrast has visually better SNR than the TD70 (window and level the same). The T1-weighted image precontrast also has higher SNR for TD150 compared with TD70 due to larger T1 recovery time. The PD-weighted reference image used the same parameters (5° readout flip angle, TR = 7.5 msec, TE = 1.48 msec, no saturation preparation pulse) for both acquisitions and thus similar SNR.

increases compared to the corresponding TD150 ones ($P < 0.01$).

DISCUSSION

It is important to recognize that the relationship between signal intensity and Gd-DTPA contrast concentration is always a nonlinear curve with saturation-prepared perfusion sequences (33). This nonlinearity has to be considered for an accurate quantitative evaluation of contrast-enhanced first-pass perfusion MRI (34). In this study, the degree of the nonlinearity affects the signal intensity in the myocardium was evaluated in healthy volunteers at rest and during stress perfusion imaging using a GRE-EPI sequence and common acquisition parameters. Based on magnetization modeling, we showed that this nonlinearity compresses the dynamic range of myocardial time signal intensity curves at peak contrast enhancement and more severely during stress than rest. This compression affects perfusion estimates and results in underestimation of MBF and myocardial perfusion reserve. We showed that nonlinear signal intensity correction methods, such as the one used here, improve semiquantitative and quantitative measures of myocardial perfusion.

We derived nonlinear conversion factors from magnetization simulations to map myocardial signal intensity to contrast concentration units as described in the Materials and Methods section. For practical implementation, this relationship can be applied as a look-up-table to correct nonlinear myocardial signal saturation in the perfusion imaging but the model needs to be derived for a specific pulse sequence and acquisition parameters.

We compared the magnitude of the nonlinear signal intensity correction using different saturation-recovery TD settings, as TD is one of the most important parameters that affects the nonlinear signal intensity response in the GRE-EPI perfusion sequence (33). As in the simulation (Fig. 1), significant signal intensity compression was observed in all TD settings at high contrast concentrations. There are important tradeoffs between SNR and linearity when choosing perfusion acquisition parameters. Despite the fact that long TD increases the myocardial signal intensity, the nonlinearity is more prominent than with a short delay. While the TD25 setting is more linear, it has lower signal intensity magnitude. Furthermore, the nonuniformity of k-space weighting in the TD25 due to saturation-recovery may lead to artifacts since the uniformity of k-space weighting will depend on both TD and readout flip angle (33).

As shown previously (18,32), quantitative analysis of myocardial perfusion is dependent on accurately assessing the peak of myocardial enhancement and contrast kinetics. In the current study, we have shown the peak portion of the myocardial time signal intensity curve is most strongly affected by signal intensity nonlinearity due to higher contrast concentration (Figure 5). Since vasodilated stress perfusion has higher signal intensity overshoots at peak enhancement than the

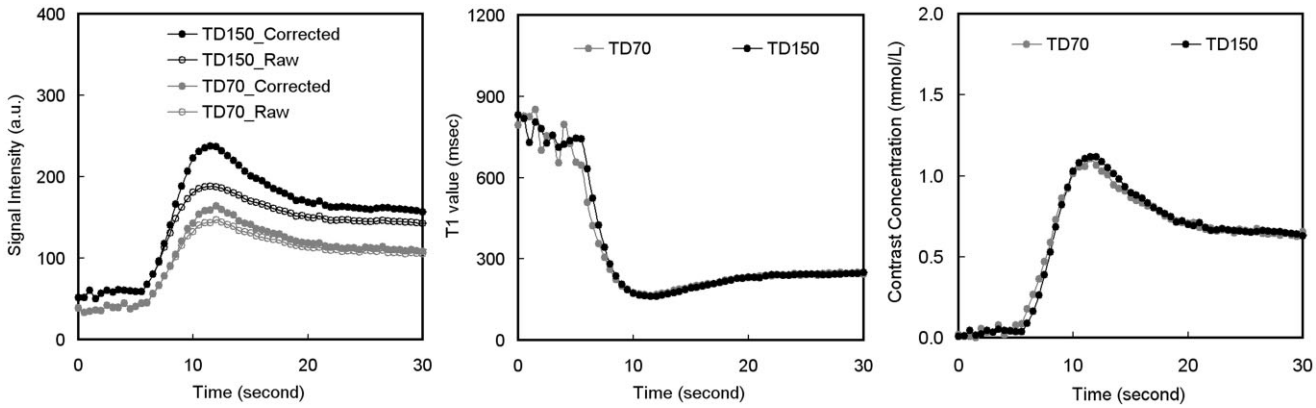

Figure 5. Comparison of stress myocardial time signal intensity curves before and after the nonlinear correction reveals more severe signal intensity compression for TD150 than the TD70 study (left), particularly at the time period near the peak myocardial contrast concentration (from 10 to 15 seconds along the time axis). The corresponding time T1 curves and time contrast concentration curves are shown in the middle and right plots for comparison.

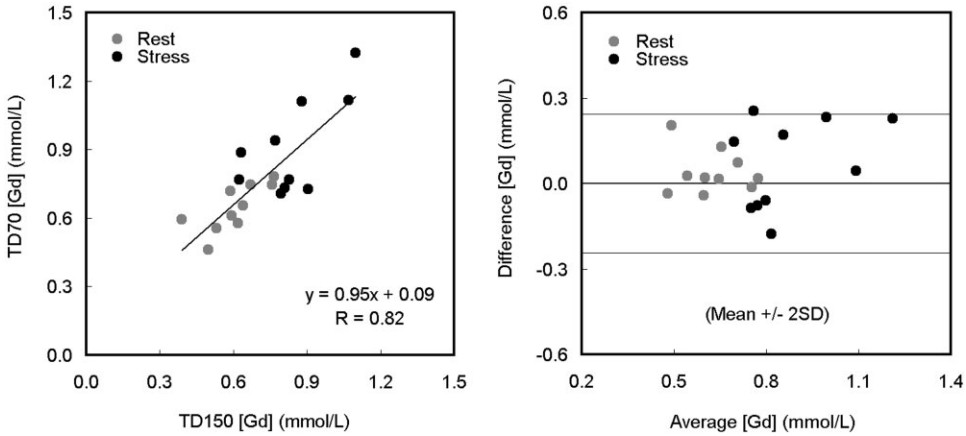

Figure 6. Peak myocardial contrast concentration estimated from TD70 and TD150 perfusion studies correlates well. Bland-Altman analysis shows no systematic difference.

corresponding rest study, the signal intensity correction has greater effects on stress perfusion and perfusion reserve than the rest study.

A few studies have shown estimates of T1 relaxivity (R1) or Gd-DTPA concentration from the time signal intensity curves of first-pass myocardial perfusion imaging in humans. These studies used either inversion-recovery (35–37) or saturation-recovery methods (16,38) to calibrate the signal intensity in terms of the contrast concentration. Based on our methods, the averaged peak myocardial contrast concentration was estimated to be 0.63 mmol $\cdot$ L^{-1} at rest and 0.87 mmol $\cdot$ L^{-1} during stress for full-dose first-pass perfusion. These peak concentration estimates fit within a range as reported by other studies (16,35).

In a separate healthy volunteer study comparing quantitative myocardial perfusion estimates using MRI and positron emission tomography (PET) (38), slight underestimation of MBF and myocardial perfusion reserve were reported from MR studies compared to the PET reference. This underestimation may partially due to the selected contrast kinetic model or model parameters, or as a direct result of signal intensity compression as here mentioned. In the current study, we used a Fermi model constrained deconvolution to estimate MBF and MPR as validated previously (18,19). The range of MBF and MPR estimates that we obtained from both TDs after the nonlinear myocardial signal intensity correction were in line with previous PET references for different healthy volunteers (6,38).

The precontrast T1 value is an important factor in the simulation and it can vary due to incomplete contrast excretion from the prior contrast administration. In this study the stress perfusion was performed at least four hours before the rest perfusion to minimize these effects but this might not be practical for patient studies. While the precontrast T1 value for all stress studies was assumed at 850 msec, the precontrast T1 value of individual rest study can be estimated at the baseline time point to compensate the residual contrast. The average difference of the precontrast T1 value in rest perfusion was found to be less than 10% compared to the corresponding stress perfusion for both TD studies. This small percent of precontrast T1 elevation should not change the nonlinear correction substantially, as seen in the Fig. 2 simulation.

In our image acquisition, we used the TSENSE technique (31) at rate 2 to permit a short imaging time and thereby reduce the nonlinearity. While the saturation-recovery TD was cited in this study as one of the important settings that affects the signal intensity nonlinearity, it should be noted that the effect of nonlinearity is actually proportional to the time elapsed to the center of k-space. The use of accelerated imaging techniques essentially shorten the acquisition time and increase the

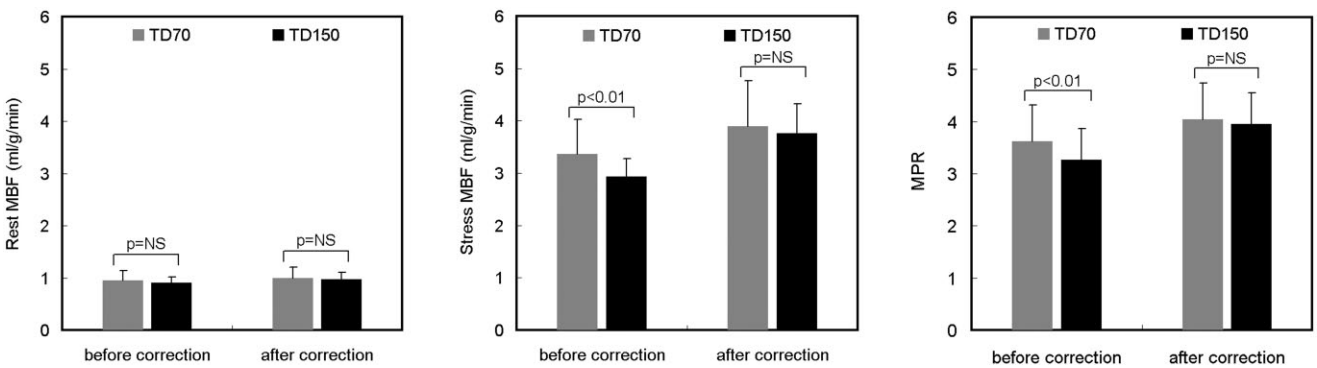

Figure 7. Stress MBF and MPR estimated by Fermi MCD for TD70 and TD150 studies were statistically different ($P < 0.01$) before the nonlinear correction, but became similar (P = NS) after the correction. Rest MBF remained similar before or after the correction (P = NS). All perfusion estimates were increased after the corrections for both TDs.

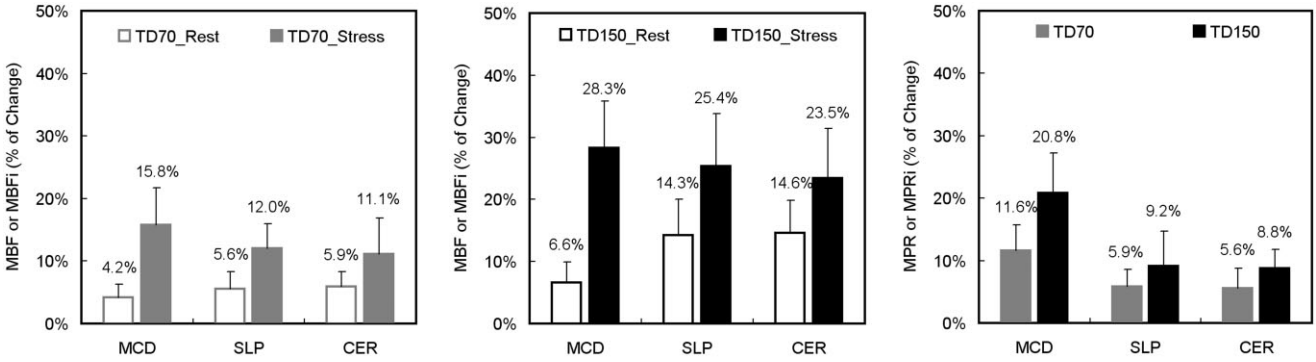

Figure 8. Magnitude of change of perfusion estimates after the nonlinear correction was compared as a function of TD and as a function of rest vs. stress study. All rest perfusion estimates had smaller increase compared with the corresponding stress measures (all $P < 0.01$). All TD70 perfusion estimates had smaller increases than the corresponding TD150 measurements (all $P < 0.01$). All perfusion estimates were increased after the correction for both TDs. MBF = myocardial blood flow, MBFi = MBF index, MPR = myocardial perfusion reserve, MPRi = MPR index, MCD = model-constrained deconvolution, SLP = intensity upslope, CER = contrast enhancement ratio.

signal linearity range for quantitative perfusion analysis (33,39).

We used a full-dose of Gd-DTPA contrast and different TD settings to study the nonlinearity of myocardial signal intensity. It is possible that a lower dose of contrast or a lower TD setting may further reduce such nonlinearity but with a tradeoff in SNR and possible image artifacts. The degree of signal intensity correction for other acquisition parameters can be expected to be more or less extreme. Thus, one can incorporate similar nonlinear signal intensity correction methods according their specific imaging sequences and protocols to improve quantitative analysis of myocardial perfusion.

In the current study, we optimized the imaging sequence to improve the accuracy of signal intensity corrections, including: 1) a PD-weighted imaging for intensity normalization, 2) composite 90° pulses (33,40) to minimize variability due to inaccuracies in flip angle, and 3) parallel imaging and EPI to shorten the acquisition time. There are still other limiting factors to the accuracy of signal intensity corrections that need to be addressed. For example, the precision of 25° and 5° readouts in the T1 and PD imaging might be affected by inaccurate scanner system calibration or B1 field inhomogeneities; a PD reference at higher flip angle without saturation preparation might be used since it might reduce the error sensitivity in actual readout flip angle.

The effect of T2 or T2* was neglected in this study because of the short echo time used. One may need to adjust the precontrast T1 and T2 values in the simulation to achieve the highest accuracy of signal intensity corrections. Heterogeneity of the gadolinium contrast concentration in the tissue is not adequately addressed by modeling at bulk magnetization level or the homogeneous fluid phantom in this study. Other physiological factors such as the extraction fraction on first-pass of the contrast may also affect perfusion quantification but the assessment is beyond the scope of this study.

In conclusion, the nonlinearity between myocardial signal intensity and gadolinium contrast concentration affects perfusion quantification in a full-dose Gd-DTPA contrast (0.1 mmol/kg) setting. This nonlinear distortion compresses myocardial time signal intensity curves and leads to underestimation of all quantitative perfusion measures studied. The effects are larger for stress than rest perfusion studies and more severe for long TD than short TD studies. However, the underestimation of perfusion measures can be rectified using a nonlinear signal intensity correction. This study showed that intrasubject quantitative MR perfusion measures estimated using different imaging parameter (TD) settings correlated well after such correction. It is feasible and efficacious to calibrate myocardial time signal intensity according to gadolinium contrast concentration, and such nonlinear signal intensity correction improves quantitative perfusion analysis.

REFERENCES

1. Plein S, Radjenovic A, Ridgway JP, et al. Coronary artery disease: myocardial perfusion MR imaging with sensitivity encoding versus conventional angiography. Radiology 2005;235:423–430.
2. Thiele H, Plein S, Breeuwer M, et al. Color-encoded semiautomatic analysis of multi-slice first-pass magnetic resonance perfusion: comparison to tetrofosmin single photon emission computed tomography perfusion and X-ray angiography. Int J Cardiovasc Imaging 2004;20:371–384.
3. Bunce NH, Reyes E, Keegan J, et al. Combined coronary and perfusion cardiovascular magnetic resonance for the assessment of coronary artery stenosis. J Cardiovasc Magn Reson 2004;6:527–539.
4. Nagel E, Klein C, Paetsch I, et al. Magnetic resonance perfusion measurements for the noninvasive detection of coronary artery disease. Circulation 2003;108:432–437.
5. Doyle M, Fuisz A, Kortright E, et al. The impact of myocardial flow reserve on the detection of coronary artery disease by perfusion imaging methods: an NHLBI WISE study. J Cardiovasc Magn Reson 2003;5:475–485.
6. Ibrahim T, Nekolla SG, Schreiber K, et al. Assessment of coronary flow reserve: comparison between contrast-enhanced magnetic resonance imaging and positron emission tomography. J Am Coll Cardiol 2002;39:864–870.
7. Schwitter J, Nanz D, Kneifel S, et al. Assessment of myocardial perfusion in coronary artery disease by magnetic resonance: a comparison with positron emission tomography and coronary angiography. Circulation 2001;103:2230–2235.
8. Panting JR, Gatehouse PD, Yang GZ, et al. Echo-planar magnetic resonance myocardial perfusion imaging: parametric map analysis and comparison with thallium SPECT. J Magn Reson Imaging 2001;13:192–200.

9. Al-Saadi N, Nagel E, Gross M, et al. Noninvasive detection of myocardial ischemia from perfusion reserve based on cardiovascular magnetic resonance. Circulation 2000;101:1379–1383.
10. Taylor AJ, Al-Saadi N, Abdel-Aty H, et al. Elective percutaneous coronary intervention immediately impairs resting microvascular perfusion assessed by cardiac magnetic resonance imaging. Am Heart J 2006;151:891–897.
11. Laham RJ, Simons M, Pearlman JD, Ho KK, Baim DS. Magnetic resonance imaging demonstrates improved regional systolic wall motion and thickening and myocardial perfusion of myocardial territories treated by laser myocardial revascularization. J Am Coll Cardiol 2002;39:1–8.
12. Al-Saadi N, Nagel E, Gross M, et al. Improvement of myocardial perfusion reserve early after coronary intervention: assessment with cardiac magnetic resonance imaging. J Am Coll Cardiol 2000; 36:1557–1564.
13. Panse P, Klassen C, Panse N, et al. Magnetic resonance quantitative myocardial perfusion reserve demonstrates improved myocardial blood flow after angiogenic implant therapy. Int J Cardiovasc Imaging 2007;23:217–224.
14. Wang L, Jerosch-Herold M, Jacobs DR Jr, Shahar E, Folsom AR. Coronary risk factors and myocardial perfusion in asymptomatic adults: the Multi-Ethnic Study of Atherosclerosis (MESA). J Am Coll Cardiol 2006;47:565–572.
15. Rosen BD, Lima JA, Nasir K, et al. Lower myocardial perfusion reserve is associated with decreased regional left ventricular function in asymptomatic participants of the multi-ethnic study of atherosclerosis. Circulation 2006;114:289–297.
16. Cernicanu A, Axel L. Theory-based signal calibration with single-point T1 measurements for first-pass quantitative perfusion MRI studies. Acad Radiol 2006;13:686–693.
17. Utz W, Niendorf T, Wassmuth R, Messroghli D, Dietz R, Schulz-Menger J. Contrast-dose relation in first-pass myocardial MR perfusion imaging. J Magn Reson Imaging 2007;25:1131–1135.
18. Christian TF, Rettmann DW, Aletras AH, et al. Absolute myocardial perfusion in canines measured by using dual-bolus first-pass MR imaging. Radiology 2004;232:677–684.
19. Hsu LY, Rhoads KL, Holly JE, Kellman P, Aletras AH, Arai AE. Quantitative myocardial perfusion analysis with a dual-bolus contrast-enhanced first-pass MRI technique in humans. J Magn Reson Imaging 2006;23:315–322.
20. Kostler H, Ritter C, Lipp M, Beer M, Hahn D, Sandstede J. Prebolus quantitative MR heart perfusion imaging. Magn Reson Med 2004; 52:296–299.
21. Ritter C, Brackertz A, Sandstede J, Beer M, Hahn D, Kostler H. Absolute quantification of myocardial perfusion under adenosine stress. Magn Reson Med 2006;56:844–849.
22. Gatehouse PD, Elkington AG, Ablitt NA, Yang GZ, Pennell DJ, Firmin DN. Accurate assessment of the arterial input function during high-dose myocardial perfusion cardiovascular magnetic resonance. J Magn Reson Imaging 2004;20:39–45.
23. Kim D, Axel L. Multislice, dual-imaging sequence for increasing the dynamic range of the contrast-enhanced blood signal and CNR of myocardial enhancement at 3T. J Magn Reson Imaging 2006;23: 81–86.
24. Vallee JP, Lazeyras F, Kasuboski L, et al. Quantification of myocardial perfusion with FAST sequence and Gd bolus in patients with normal cardiac function. J Magn Reson Imaging 1999;9:197–203.
25. Giang TH, Nanz D, Coulden R, et al. Detection of coronary artery disease by magnetic resonance myocardial perfusion imaging with various contrast medium doses: first European multi-centre experience. Eur Heart J 2004;25:1657–1665.
26. Wolff SD, Schwitter J, Coulden R, et al. Myocardial first-pass perfusion magnetic resonance imaging: a multicenter dose-ranging study. Circulation 2004;110:732–737.
27. Ding S, Wolff SD, Epstein FH. Improved coverage in dynamic contrast-enhanced cardiac MRI using interleaved gradient-echo EPI. Magn Reson Med 1998;39:514–519.
28. Sekihara K. Steady-state magnetizations in rapid NMR imaging using small flip angles and short repetition intervals. IEEE Trans Med Imaging 1987;6:157–164.
29. Harrison R, Bronskill MJ, Henkelman RM. Magnetization transfer and T2 relaxation components in tissue. Magn Reson Med 1995; 33:490–496.
30. Stanisz GJ, Henkelman RM. Gd-DTPA relaxivity depends on macromolecular content. Magn Reson Med 2000;44:665–667.
31. Kellman P, Epstein FH, McVeigh ER. Adaptive sensitivity encoding incorporating temporal filtering (TSENSE). Magn Reson Med 2001; 45:846–852.
32. Jerosch-Herold M, Seethamraju RT, Swingen CM, Wilke NM, Stillman AE. Analysis of myocardial perfusion MRI. J Magn Reson Imaging 2004;19:758–770.
33. Kellman P, Arai AE. Imaging sequences for first pass perfusion—a review. J Cardiovasc Magn Reson 2007;9:525–537.
34. Heilmann M, Kiessling F, Enderlin M, Schad LR. Determination of pharmacokinetic parameters in DCE MRI: consequence of nonlinearity between contrast agent concentration and signal intensity. Invest Radiol 2006;41:536–543.
35. Larsson HB, Fritz-Hansen T, Rostrup E, Sondergaard L, Ring P, Henriksen O. Myocardial perfusion modeling using MRI. Magn Reson Med 1996;35:716–726.
36. Fritz-Hansen T, Rostrup E, Larsson HB, Sondergaard L, Ring P, Henriksen O. Measurement of the arterial concentration of Gd-DTPA using MRI: a step toward quantitative perfusion imaging. Magn Reson Med 1996;36:225–231.
37. Vallee JP, Sostman HD, MacFall JR, et al. MRI quantitative myocardial perfusion with compartmental analysis: a rest and stress study. Magn Reson Med 1997;38:981–989.
38. Parkka JP, Niemi P, Saraste A, et al. Comparison of MRI and positron emission tomography for measuring myocardial perfusion reserve in healthy humans. Magn Reson Med 2006;55:772–779.
39. Weber S, Kronfeld A, Kunz R, Fiebich M, Kreitner K, Schreiber W. Comparison of three accelerated pulse sequences for quantitative myocardial perfusion imaging using TSENSE. In: Proceedings of the 14th Annual Meeting of ISMRM, Seattle, WA, USA, 2006 (Abstract 206).
40. Oesingmann N, Zhang Q, Simonetti O. Improved saturation RF pulse design for myocardial first pass perfusion at 3T. J Cardiovasc Magn Reson 2004;6:373–374.